Research Article

Abdullah F. Al Asmari, Muhammad Iqbal Bashir, Furqan Farooq*, and Usama Asif

Investigating the effect of locally available volcanic ash on mechanical and microstructure properties of concrete

https://doi.org/10.1515/rams-2024-0085
received March 18, 2024; accepted December 27, 2024

Abstract: Environmental degradation is developing due to rising pollution from the depletion of raw materials and the growing mandate for concrete goods. Investigators and experts have focused on creating sustainable concrete utilizing renewable elements. Volcanic ash (VA) is a promising supplementary cementitious material among these minerals. Therefore, it is crucial to examine the attributes of voids in aggregate and how they impact the performance of concrete. VA from the Gini Chilas (Gigilat Baltistan) was used to prepare specimens. Mixing regimes of VA concrete with altering concentrations ranging from 0 to 40% replacement was cast. Water-to-cement ratio was reserved persistent for all the mixes. Chemical compositions of VA and properties of concrete in relation to workability, density, and compressive strength were carried out. In addition, thermo-gravimetric analysis, scanning electron microscope (SEM), and X-ray diffraction analysis were also examined. The analysis of results reveals that VA with 10% replacement gives an adamant response. This is due to the natural pozzolanic effect that details the creation of additional dense gel (C–S–H), and deviation of cracks is observed from SEM. VA_{10} also exhibits thermally stable behavior at temperature with less percentage mass loss. However, VA up to 10% replacement in cementitious concrete can exhibit better properties than normal specimens.

Keywords: compressive strength, scanning electron microscope, thermo-gravimetric, volcanic ash, workability, and X-ray diffraction

*** Corresponding author: Furqan Farooq,** NUST Institute of Civil Engineering (NICE), School of Civil and Environmental Engineering (SCEE), National University of Sciences and Technology (NUST), Sector H-12, Islamabad, 44000, Pakistan; Western Caspian University, Baku, Azerbaijan, e-mail: ffarooq.ms15@nice.nust.edu.pk

Abdullah F. Al Asmari: Civil Engineering Department, College of Engineering, King Khalid University, Abha, 61421, Saudi Arabia, e-mail: Afsaeed@kku.edu.sa

Muhammad Iqbal Bashir: Department of Civil Engineering, University of Engineering and Technology, Taxila, 47050, Pakistan, e-mail: Iqbal833@yahoo.com

Usama Asif: Department of Civil and Environmental Engineering, School of Engineering and Digital Sciences, Nazarbayev University, Nur-Sultan, 010000, Kazakhstan; Department of Civil and Environmental Engineering, University of Maryland, College Park, MD 20742, United States, e-mail: usama.asif@nu.edu.kz

1 Introduction

Concrete is often regarded as the predominant construction material, exhibiting a substantial global use estimated to be in the billions of cubic meters worldwide [1–4]. Moreover, the outcome of cement is seeing significant increases in direct correlation with the consumption of concrete [5]. Nevertheless, it is worth noting that the cement production process, particularly during the grinding and clinker burning stages, is associated with significant levels of greenhouse gas emissions (GHGs) [6]. The manufacture of cement is accountable for around 6% of global carbon dioxide (CO_2) emissions, thus contributing to the phenomenon of global warming [7]. Furthermore, the production of cement is responsible for 95% of the total CO_2 production associated with the manufacturing of one cubic meter of concrete [8]. The Portland cement (PC) industry is acknowledged as a significant contributor to global CO_2 emissions, accounting for an estimated 5–7% of the total emissions [9–11]. In addition, the annual global production of cement falls between 2.8 and 4.1 billion tons. It is reported that the production of PCs amounts to 4,000 million tons yearly and is projected to increase to around 6,000 million tons by the year 2060 [12]. These figures mentioned above can be further diminished through the augmentation of alternative materials in the process of concrete manufacture [13–18]. Therefore, the cement industry exhibits a rather high level of pollution in the atmosphere. Moreover, it is imperative to utilize financial strategies that can serve as viable substitutes for cement. Therefore, the implementation of these approaches results in a decrease in the utilization of cement within

Open Access. © 2025 the author(s), published by De Gruyter. This work is licensed under the Creative Commons Attribution 4.0 International License.

concrete mixtures [14]. Researchers conducted studies to explore the potential of utilizing industrial by-products and waste materials in concrete as a means of environmental conservation to develop green concrete [19–25]. Therefore, to reduce clinker production and CO_2 emissions, supplementary cementitious materials (SCMs) such as fly ash (FA) [26–28], silica fume (SF) [29–31], electronic arc furnace slag [32–34], rice husk ash (RHA) [35–37], wheat straw ash [38–40], and ordinary pozzolans are employed as substitutes for cement. These materials lack inherent binding qualities and are considered the most cost-effective alternatives to cement [41]. Hence, the incorporation of these materials can result in a decrease in the proportion of ordinary Portland cement (OPC) used in the manufacturing of concrete. The utilization of SCMs in the manufacturing of cement concrete offers additional environmental advantages. This practice mitigates the accumulation of excessive waste in open areas and landfills, which is known to contribute to environmental contamination and pose risks to human health. Furthermore, the incorporation of their presence inside cementitious composites (CCs) enhances various properties in the matrix, as depicted in Figure 1.

Durable building material SCMs can originate after manufacturing waste such as slag, FA, and ground granulated blast-furnace slag, as well as cultivated waste such as RHA and palm oil fuel ash [39]. The aforementioned SCMs demonstrate a notable degree of pozzolanic reactivity and fall under the classifications of natural pozzolans. Hence, these materials possess the potential to serve as limited substitutes for cement. This results in the attainment of cement mortar with acceptable performance or even concrete with enhanced performance [9]. Hence, the utilization of pozzolans as a substitute for cement in concrete blends leads to a substantial reduction in GHGs that are sent into the environment [1,2,42,43]. The utilization of natural pozzolanas as a partial replacement for PC has been extensively practiced in many applications. This is primarily attributed to the presence of reactive SiO_2 in natural pozzolanas, which imparts several advantageous properties such as diminished heat generation, reduced permeability, and enhanced resistance to chemical deterioration in the CC. Therefore, it is possible to utilize abundant certainly occurring pozzolanic materials [3,44–46], such as volcanic ash (VA) [47–49], volcanic pumice [50–52], and calcined clay [53–55], as a viable substitute to fulfill the requirements of the concrete industry.

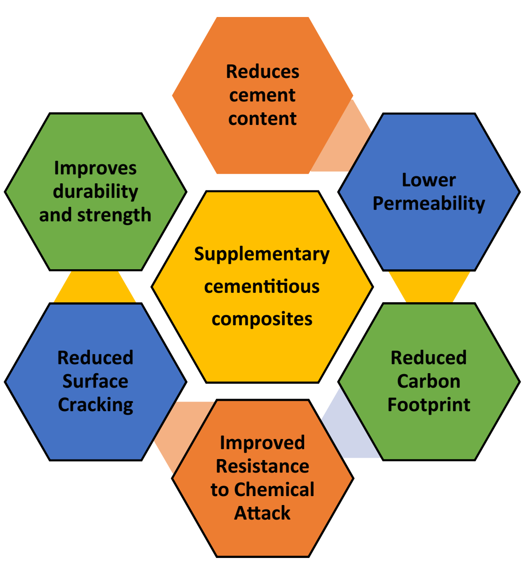

Figure 1: SCM benefits in CC.

Volcanic concrete is an environmentally friendly material that incorporates components derived from naturally occurring igneous volcanic rock [56–58]. When volcanic rock is crushed into various particle sizes, it can be utilized as coarse aggregate, fine aggregate, or as a SCM in concrete production. VA offers significant environmental advantages compared to other SCMs, such as FA and slag. As a naturally available material, VA requires minimal processing, resulting in lower energy consumption and reduced carbon emissions. In contrast to FA, a byproduct of coal combustion, and slag, a byproduct of steel manufacturing, VA is not reliant on industrial processes, making it a more sustainable alternative. Its natural abundance in certain regions also reduces transportation needs, lowering the overall environmental impact. By partially replacing cement, VA helps decrease CO_2 emissions in concrete production, contributing to more sustainable construction practices.

VA is a non-reactive siliceous pozzolanic substance that, when mixed with lime and water, produces a cementitious material with exceptional structural properties. The substance can efficiently occupy the empty voids among the bigger particles [57]. Thus, it diminishes the exothermic reaction of hydration and undergoes a chemical reaction with calcium hydroxide $Ca(OH)_2$, resulting in the formation of calcium silicate hydrate [56]. Several academic studies have analyzed how ordinary VA affects the mechanical and microstructural properties of mortar and concrete. Sebayang [59] investigated the effect of the utilization of VA in concrete and reported a significant improvement of 9.8% in compressive strength and 5.99% in tensile strength, respectively. In addition, Karolina and Simanjuntak [60] revealed that the workability of concrete is reduced with an increase in the ratio of VA as a substitute for cement. Hossain and Lachemi [61] demonstrated that a compressive strength of 60 MPa was attained after 28 days when 20% volume of admixture (VA) was used as a substitute for cement. Furthermore, their findings indicated that the optimal ratio for incorporating VA was determined to be 5%, regardless of the range of VA concentrations tested, which spanned from 0 to 20%. Khan *et al.* [62] demonstrated that the pozzolanic activity exhibited an upward trend in correlation with the degree of fineness of the material. Nevertheless, the use of heat treatment on VA yielded unfavorable results. Abdullah *et al.* [63] conducted a study that revealed the positive impact of volcanic pumice stone ash on the compressive strength of self-compacting concretes. This finding highlights the significance of the fineness level of VAs to the mechanical properties of such concretes. Al-Fadala *et al.* [64] investigated the effect of VA with varying concentrations ranging from 10 to 30% in cementitious matrix. The author reveals that the inclusion of VA at a 10% replacement level in cement led to a little decrease in quality. In contrast, the incorporation of VA in cement at replacement ratios of 20 and 30% resulted in notable decreases in strength as associated to the resistor samples. Additionally, the incorporation of VA powder as a partial substitute for OPC has been shown to result in reduced water absorption, sportively, and void content, as well as enhanced resistance to acid and sulfate assault, chloride permeability, and other factors, when compared to conventional concrete [65,66]. Al-Bahar *et al.* [67] discovered that the substitution of 10–30% of OPC with VA leads to a notable enhancement in both the mechanical and microstructural characteristics of cement paste. Moreover, the durability properties of volcanic ash concrete (VAC) were examined by Hossain and Lachemi [68,69]. Their investigation encompassed the evaluation of fresh, hardened, and durability characteristics. The findings of their study indicate that VAC exhibits superior durability capabilities in comparison to the control concrete sample containing 0% VA. Nevertheless, increasing the concentration of VA has a malignant consequence on the strength of VAC. Celik *et al.* [66] successfully formulated a high-volume natural pozzolanic concrete, which involved replacing 45% of OPC. The resulting matrix substantially exhibited a 28-day compressive strength of 34 MPa. Liu *et al.* [70] studied the impact of VA on the thermal stability of asphalt. The author indicated that the inclusion of VA led to enhancements in the mechanical characteristics of asphalt mixtures. Previous research studies have shown evidence that mechanical, chemical, and thermal treatments can enhance the properties of natural pozzolans. Additionally, the significance of VA in concrete is illustrated by a scientometric graphic, as presented in Figure 2. However, large-scale adoption of VA faces challenges, such as variations in its chemical composition, which can affect performance consistency in concrete. Additionally, in regions where VA is not readily available, transportation costs may hinder its widespread use.

The objective of this research was to examine the impact of incorporating VA as an auxiliary for cement in the production of a CC. The variable concentration of VA is

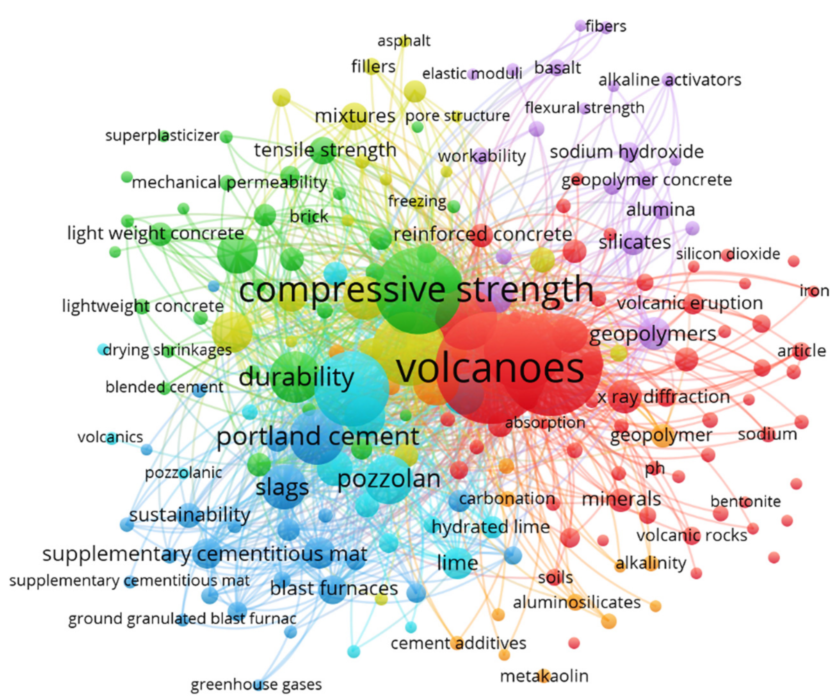

Figure 2: Scientometric diagram of VA.

substituted with a range spanning from 0 to 40%. The evaluation of fresh and hardened qualities is initially performed through experimental tests, specifically focusing on workability, density, and compressive strength. In addition, VAC specimens are subjected to a temperature range of 0–900°C to assess the effects on the pozzolanic material. The chemical analysis of VA concrete is performed using X-ray fluorescence (XRF) and X-ray diffraction (XRD) analysis techniques. Furthermore, a comprehensive analysis of the mixes was performed using XRD and thermogravimetric analysis (TGA) methods to assess the influence of VA on the microstructure of the CC.

Table 1: Chemical composition of cement and VA

Oxide	VA (% age by mass)	PC (% age by mass)
SiO_2	53.69	21.5
Al_2O_3	17.43	6.00
Fe_2O_3	9.52	3.75
CaO	7.00	62.00
MgO	3.87	2.8
Na_2O	3.57	0.2
K_2O	0.86	1.00
SO_3	0.16	2.75
Lime saturation factor	3.89	96.40
Silica modulus	1.99	2.5
Aluminum modulus	1.83	1.25
LOI	1.3	6.64

2 Materials and methods

2.1 Materials

For the manufacture of specimens, OPC Type 1 Grade 42.5-N and natural sand conforming to ASTM C150 [71] and ASTM C128 [72] standards were utilized. The VA used in this study was sourced from Gini Chilas, located in Gilgit Baltistan, Pakistan, as shown in Figure 3. This particular source was chosen due to its accessibility, abundance, and established history of local use in construction. Additionally, it was selected based on the initial chemical analysis, which indicated suitable pozzolanic activity for use in concrete mixtures. The chemical composition of the cement and VA was analyzed using XRF, with results presented in Table 1. Tables 2 and 3 show the physical properties of the materials used in the VAC mix.

It is important to note that the properties of VA can vary depending on the source due to differences in mineral composition, geographic location, and volcanic activity. If VA from other regions was used, the results of the concrete's mechanical and durability properties could differ. Variability in silica, alumina, and other oxide contents, as well as particle fineness, could affect the pozzolanic reaction, leading to variations in the concrete's strength development, workability, and overall performance.

Figure 3: VA specimen.

2.2 Mix proportions and methods

A comprehensive set of 81 samples was prepared with distinct mix proportions. These formulations include a control sample that exclusively utilized cement as a binder. A water-to-cement ratio of 0.5 was employed for all the mixtures. Table 4 provides comprehensive information regarding the mix proportion and laboratory testing conducted on all the formulations at various ages. The ingredients of the formulation were mixed in a pan mixer. Initially, the mixer was filled with both fine and coarse materials, which were then followed by the addition of cement. A period of 1 min was allocated for the dry mixing of the ingredients, with a rotational speed of 180 revolutions per minute (rpm) at a slow rate. Subsequently, a quantity equivalent to half of the total volume of water was introduced into the mixture, with the

Table 2: Physical properties of ingredients

Characteristics	Cement	VA
Insoluble residue (% mass)	0.55	—
Specific gravity ($g \cdot cm^{-3}$)	3.15	2.67%
Specific surface area ($m^2 \cdot g^{-1}$)	0.83	—
Particle size (d_{50}) (μm)	16.58	—
loss on ignition (% mass)	2.21	—
Soundness	No expansion	No expansion

Table 3: Physical and chemical properties of aggregates

	Fine aggregate		
	Physical properties		Chemical composition
Size (mm)	—	CaO	9.97
Specific gravity (g·cm^{-3})	2.64	SiO_2	49.12
Water absorption (%)	1.62	Al_2O_3	2.48
Bulk density (kg·m^{-3})	1,546		—
Crushing value	—	Fe_2O_3	38.97
Fineness modulus	2.25	K_2O	1.24

Table 4: Concrete mix proportions

Concrete mix composition					
Mixes	**Cement (kg·m^{-3})**	**VA (kg·m^{-3})**	**Water (kg·m^{-3})**	**Fine aggregate (kg·m^{-3})**	**Coarse aggregate (kg·m^{-3})**
Control sample	320	0	160	640	1,280
V_5	304	16	160	640	1,280
V_{10}	288	32	160	640	1,280
V_{15}	272	48	160	640	1,280
V_{20}	256	64	160	640	1,280
V_{25}	240	80	160	640	1,280
V_{30}	224	96	160	640	1,280
V_{35}	208	112	160	640	1,280
V_{40}	192	128	160	640	1,280

ongoing process of stirring being maintained at its original velocity for an additional duration of 2 min. Subsequently, the addition of the VA was carried out, followed by the introduction of the remaining water. The mixing process was then extended for 3 min, maintaining a rotational speed of 360 revolutions per minute (rpm). Initially, the slump test was conducted according to ASTM C143 [73], immediately after mixing, to assess the workability of fresh concrete. For compressive strength testing, 81 cylindrical specimens (100 mm × 200 mm) were prepared, with nine specimens for each mix. After demolding at 24 h, specimens were cured at 23°C and 95% humidity. Compressive strength tests were carried out at 7, 14, and 28 days, following ASTM C39 [74].

2.3 Test methods

2.3.1 Slump test for VAC

Slump tests were passed according to ASTM C143 [73] to determine the consistency of the mixes. The workability of fresh concrete was assessed by the slump test, which involved utilizing a steel cone with certain dimensions: a top diameter of 100 mm, a bottom diameter of 200 mm, and a height of 300 mm. Consistency in the slump testing was ensured by using the same water-to-cement ratio and mixing procedures for all batches, regardless of VA concentration, with experienced personnel conducting the tests to maintain accuracy.

2.3.2 Tests for hardened concrete

Hardened VAC was evaluated and compared with OPC concrete by conducting tests for dry density and compressive strength following ASTM criteria [74,75].

2.3.3 XRD

XRD spectra of specimens were obtained by using a JPX 3522 JEOL with a sensitive detector. The finely ground samples of the specimens were placed in metal sample holders and inserted into the diffractometer. XRD measurements were conducted using Cu Kα radiation with a wavelength of 1.54 Å, at 40 mA and 40 kV. XRD data were collected using a continuous scan mode with 2θ angles ranging from 0 to 160°. To ensure accuracy, calibration was performed using a standard silicon sample, which is widely accepted for calibrating XRD instruments. The calibration ensured that peak positions and intensities were accurate and reliable. While XRD effectively identifies crystalline phases, it has limitations in detecting amorphous materials, which may be significant in VA. Additionally, small quantities of crystalline phases might not be accurately identified due to XRD's detection limit.

2.3.4 TGA

TGA was utilized to measure the quantity of calcium hydroxide (CH), identify other phases in the cement pastes, and assess the extent of pozzolanic reactions. TGA was conducted using a STA 8000 Perkin Elmer instrument from the USA, which can measure mass changes as small as 1 µg. The apparatus was controlled using a dynamic heating ramp of 10°C·min^{-1} between 30 and 1,000°C. The samples were crushed to a size of 0.4 µm without any additional preprocessing to prevent destabilization of hydrates. The test was conducted in a nitrogen atmosphere provided at a flow rate of 60 mL·min^{-1}. TGA was used to measure calcium hydroxide (CH) content, identify other phases in cement pastes, and assess pozzolanic reactions. The analysis was performed with a STA 8000 Perkin Elmer instrument, capable of detecting mass changes as small as 1 µg. The apparatus operated with a dynamic heating ramp of 10°C·min^{-1} between 30 and 1,000°C. Samples were crushed to a size of 0.4 µm, and the test was conducted in a nitrogen atmosphere at a flow rate of 60 mL·min^{-1}. TGA provides insight into the thermal stability of phases but may struggle to distinguish between phases with similar decomposition temperatures. Additionally, sample preparation (such as crushing) could introduce artifacts, potentially affecting the accuracy of the analysis.

2.3.5 Microstructural analysis of VAC

The concrete sample' microstructure was analyzed with a scanning electron microscope (SEM). SEM examination was conducted at Peshawar University, Pakistan, using a JEOL-JSM 5910LV microscope with a magnification range of 0× to 300× and a maximum resolving power of 2.3 nm. The samples for SEM analysis of concrete specimens were extracted from the fractured particles of specimens subjected to compressive strength testing. The samples were sliced to a diameter of 20 mm and a height of 10 mm. The samples were kept in the laboratory under ambient conditions for 7 days to ensure that they were well dry before being coated with gold for SEM imaging.

3 Results and discussion

The chemical composition of unprocessed VA, as determined by XRF investigation, is presented in Table 1. The principal elements found in VA are silica (SiO_2), alumina (Al_2O_3), iron oxide (Fe_2O_3), calcium oxide (CaO), and magnesia (MgO). Silica has the highest weight content, with a value of 47.02 wt%. The combined percentage of SiO_2, Al_2O_3, and Fe_2O_3 is approximately 70%, indicating that VA meets the minimal criteria established by ASTM C618-15 [76] for natural pozzolans.

3.1 Workability

Figure 4 illustrates the feasibility of incorporating VA into CCs. The data reveal that the slump of volcanic concrete varied from 39 to 75 mm as the replacement level of VA increased. Furthermore, Table 1 shows a decline in workability as VA concentrations increased. This reduction in workability can be attributed to the increased water absorption capacity of VA due to its smaller particle size. Additionally, VA exhibits rough-edged polygonal particles, unlike the generally rounded particles found in cement. This shape difference may result in reduced wetting and increased inter-aggregate frictional resistance. As a result, the reduction in free water content while maintaining a consistent water-to-cement (W/C) ratio leads to decreased workability, as VA absorbs more water, reducing fluidity.

To address this, several strategies can improve workability in mixes with high VA concentrations. Adding

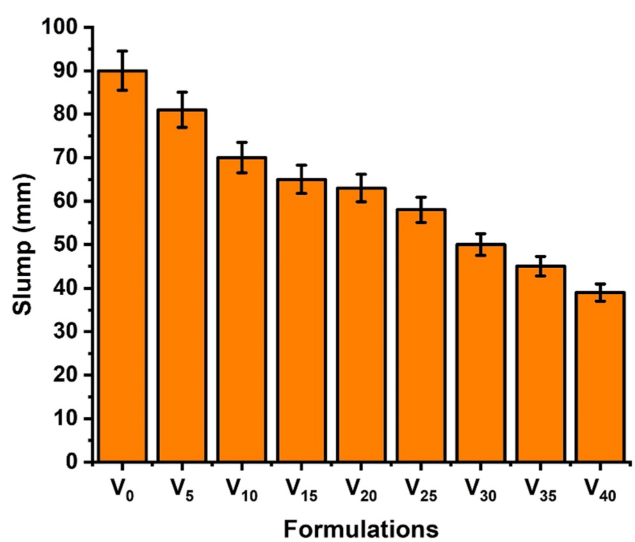

Figure 4: Slump test of intruded VA in concrete.

superplasticizers or other water-reducing admixtures can significantly enhance fluidity without altering the W/C ratio. These admixtures counterbalance the increased water absorption and frictional resistance by dispersing the cement particles more effectively, thus improving flowability [77]. Additionally, using finer VA particles or pre-wetting the ash before mixing may mitigate workability issues by reducing water absorption during mixing [78].

3.2 Density

The density of concrete plays a crucial role in influencing its mechanical properties and durability. Higher-density concrete generally exhibits enhanced strength, reduced porosity, and lower permeability to water and chemicals, contributing to increased durability and longer service life. As shown in Figure 5, the series of concrete mixtures containing VA demonstrated slightly higher densities compared to the reference concrete after a 28-day curing period. This increase in density can be attributed to the filler effect of VA, which fills the pores within the concrete matrix, improving compactness by freeing trapped water. Silva *et al.* [79] also highlighted the limited filler capacity of materials used as cement substitutes, indicating that beyond a certain threshold, further increases in density may not occur. However, in this study, the VA-enhanced particle arrangement contributed to the observed increase in density, which in turn resulted in enhanced strength and durability.

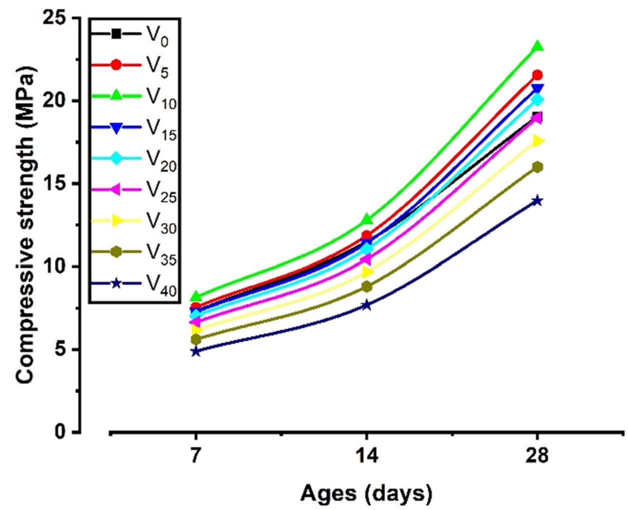

Figure 6: Compressive strength of VAC.

3.3 Compressive strength of VAC

The compressive strength data for concrete reinforced with nano media at various time intervals are presented in Figure 6. The compressive strength of the VA concrete exhibited superior performance compared to the reference sample, up to a concentration of 10%. The compressive strength exhibits an initial increase followed by a subsequent drop in comparison to the control sample. The observed increase in strength can be due to the presence of reactive silica and alumina in VA, which have the potential to undergo pozzolanic reactions with calcium hydroxide (lime) generated during the hydration process of PC. These reactions have a role in the generation of SCMs. Consequently, this leads to an improvement in the overall

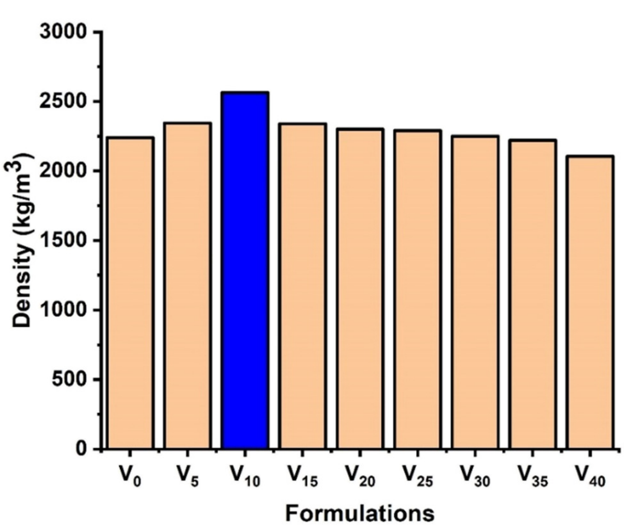

Figure 5: Formulation density.

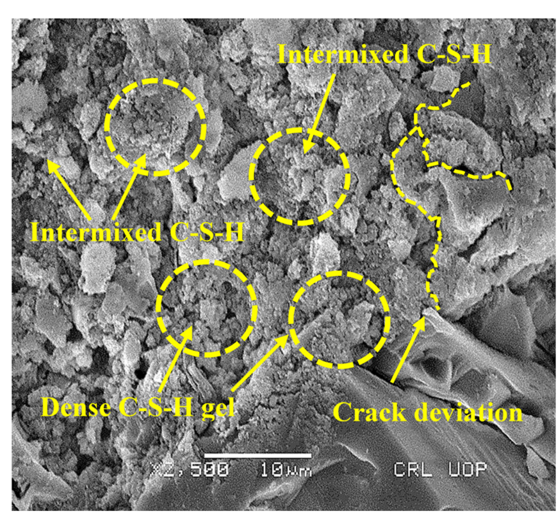

Figure 7: SEM of VA with 10% concentration.

structural integrity of the concrete material. Furthermore, the particle size and distribution of VA have the potential to influence the arrangement of particles inside the concrete mixture. An ideal configuration for packing can result in enhanced density and heightened strength. Nevertheless, the presence of large quantities of tiny particles of volcanic ash (VA) and unreactive silica might give rise to complications, including heightened water requirements and diminished workability. As a result, this leads to a detrimental effect on the overall strength. Furthermore, the SEM analysis of the V10 sample is illustrated in Figure 7. The infiltration of VA occurs within an extremely compact and dense C–S–H gel. The increased density of the gel structure has a significant role in enhancing the overall strength of the concrete. Additionally, deviations from the conventional linear crack patterns have been noticed.

3.4 Analysis of XRD of VA-based concrete

The assessment of the impact of VA on concrete is conducted by using XRD analysis, a technique that aids in the identification and characterization of its crystalline or pozzolanic properties, as illustrated in Figure 8. The control sample depicts the presence of high $Ca(OH)_2$ as compared to the remaining formulations, as shown in Figure 8(a). In addition, the presence of amorphous and glassy silica in VA undergoes a transformation into calcium–silicate–hydrate (C–S–H) upon interaction with portlandite, a constituent of cement. During the process of pozzolanic reactions, the ash particles undergo a combination with the $Ca(OH)_2$ phase present in the cement matrix. This combination results in the formation of supplementary C–S–H gels, as illustrated in Figure 8(b) and (c). The

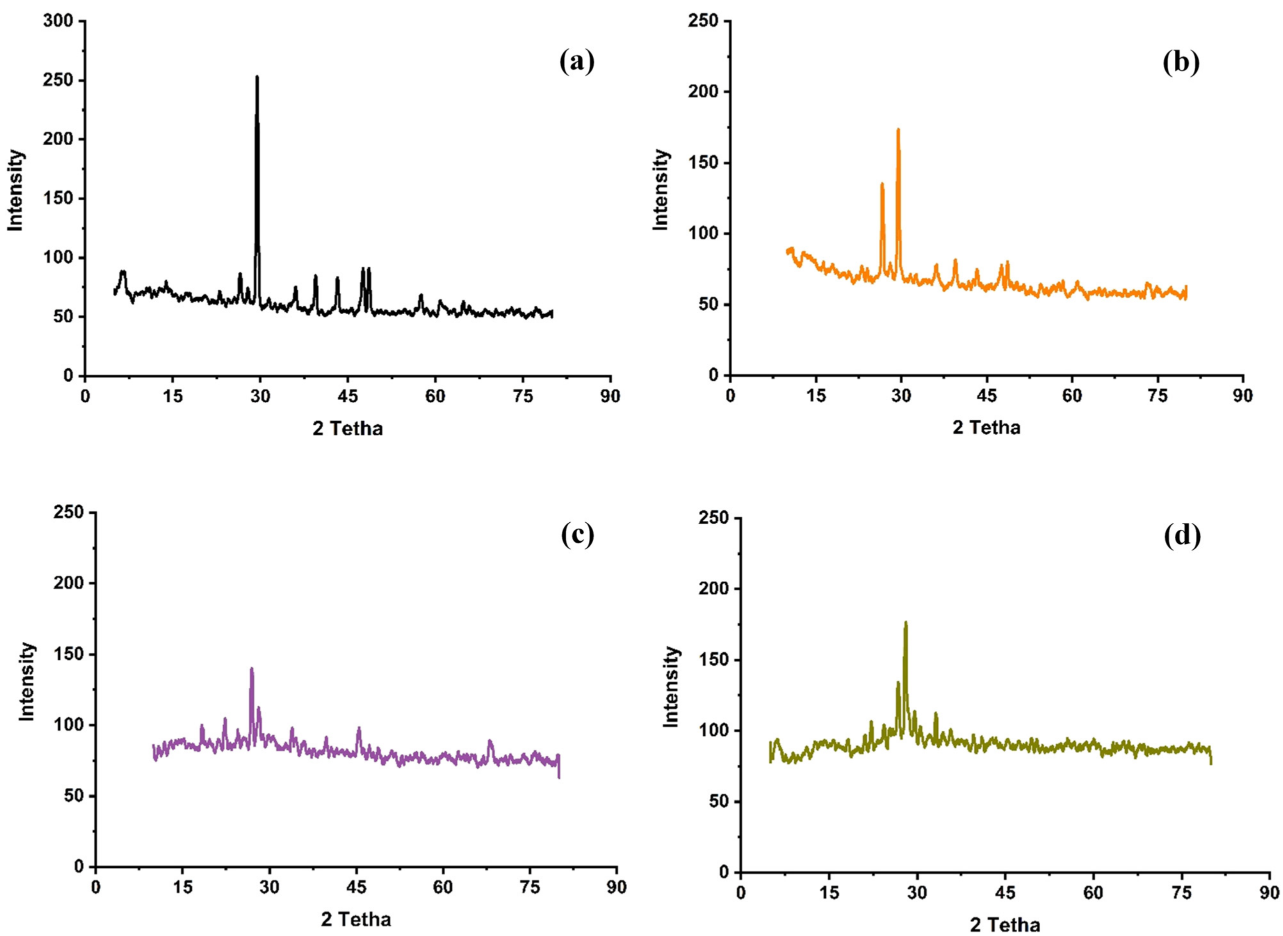

Figure 8: XRD: (a) control specimen; (b) VA with 10% replacement; (c) VA with 20% replacement; and (d) VA with 40% replacement.

augmentation of additional C–S–H gels in this production process contributes to the enhancement of the concrete's mechanical strength. Therefore, the decrease in the presence of the portlandite phase within the cement paste can be utilized as a reliable signal to assess the pozzolanic capacity of different cement materials. The control concrete sample demonstrates a significantly elevated $Ca(OH)_2$ intensity in comparison to the remaining samples. The reason for this is that the control samples consist of a notable proportion of cement, which plays a crucial role in the process of hydration and the creation of $Ca(OH)_2$. On the contrary, an inverse relationship was observed between the fraction of VA and the level of $Ca(OH)_2$ in the remaining samples. The observed reduction in $Ca(OH)_2$ concentration can be attributed to either the inert properties of VA or the limited presence of cement in these particular mixes as demonstrated in Figure 8(d). As a result, this phenomenon results in a decline in compressive strength beyond the appropriate dosage of VA.

3.5 Microstructure analysis of VA-based concrete

VA has been identified as a pozzolanic material capable of enhancing the strength and durability of concrete, as shown in Figure 9. The control sample, illustrated in Figure 10(a), exhibits fractures and voids, which lead to reduced strength and density. These inherent flaws in the microstructure compromise the concrete's workability, strength, and durability by creating pathways for the ingress of water and corrosive chemicals, ultimately reducing its lifespan.

In contrast, the microstructural improvement observed when 10% of the cement is replaced with VA, as depicted in Figure 9(b), highlights the formation of a compact and dense C–S–H gel. The pozzolanic reaction between the reactive silica in VA and calcium hydroxide generated during cement hydration results in the development of supplementary C–S–H, contributing to increased strength and durability.

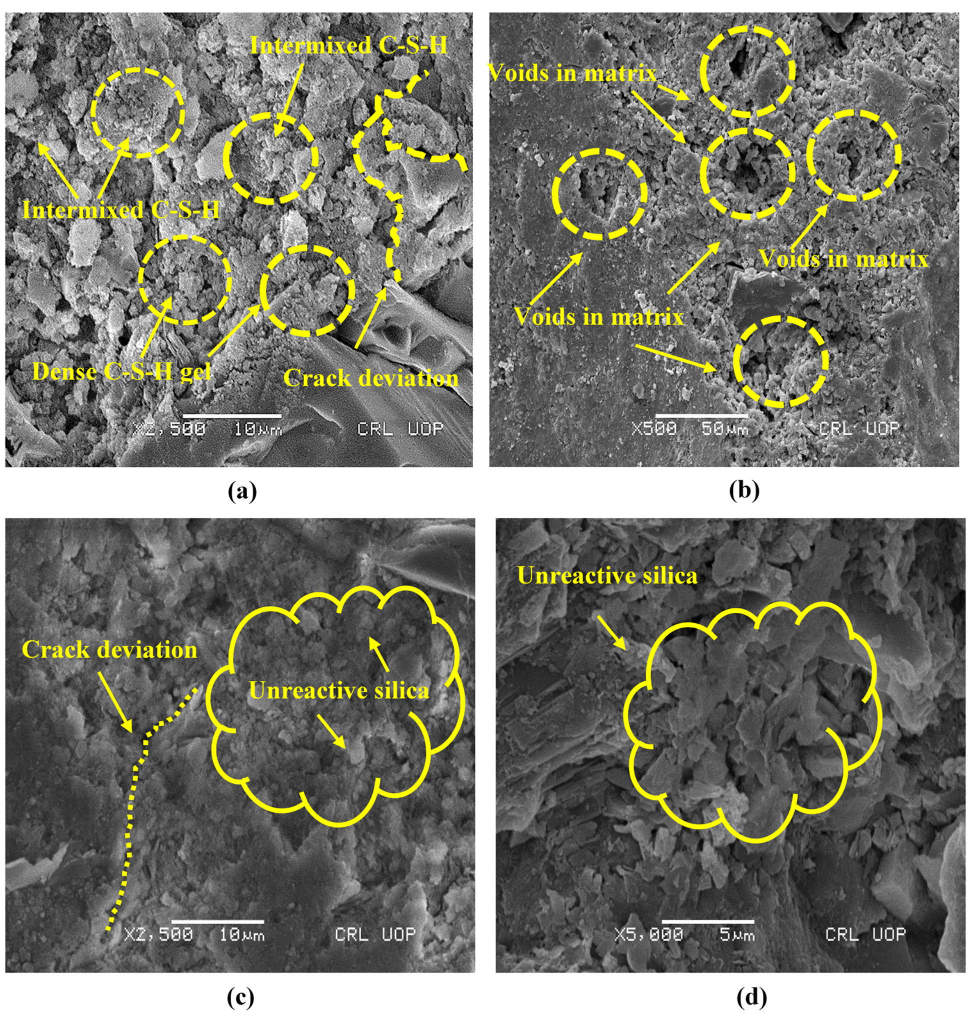

Figure 9: VAC specimens: (a) control specimen; (b) 10% VA; (c) VA with 20% replacement; and (d) VA with 40% replacement.

The enhanced gel structure reduces porosity, while the irregular morphology and coarse surface of VA particles hinder crack propagation. As cracks encounter the non-uniform VA particles, they deviate from linear paths, leading to improved resistance to cracking and enhancing the overall structural integrity [80].

However, when the VA content exceeds the optimal replacement level, as shown in Figure 9(c) and (d), the compressive strength of the concrete decreases. This reduction can be attributed to the presence of unreactive silica, a weak interfacial transition zone, and the formation of voids in the microstructure. Excessive VA particles may absorb more water, leading to increased porosity and compromised mechanical properties.

When compared to other SCMs, such as FA or SF, VA exhibits a similar pozzolanic reaction but with distinct characteristics. FA typically offers better workability due to its spherical shape, while SF can enhance compressive strength but may reduce workability. Although VA improves durability and strength to a certain extent, higher concentrations can compromise workability, akin to the effects observed with SF. However, VA's rough texture and larger particle size compared to SF can influence its effectiveness as a filler material [81].

Additionally, the particle size of VA plays a significant role in determining the microstructural properties of the concrete. Smaller VA particles tend to exhibit higher pozzolanic reactivity, which leads to more C–S–H gel formation and increased strength. Conversely, larger VA particles may act as inert fillers, reducing the effectiveness of the cementitious matrix and increasing porosity. Achieving an optimal balance between reactivity and packing density is crucial for maximizing performance benefits.

3.6 TGA of VA specimens

The TGA quantified the $Ca(OH)_2$ content in the specimens by analyzing the weight loss during thermal decomposition between 100 and 800°C, as shown in Figure 10. The TGA data indicate that the controller mix exhibited the highest concentration of portlandite (C–H) compared to the further mixtures. Furthermore, specimens through a 10% volume of VA exhibit a notable decrease in the portlandite phase due to the high responsiveness of the well-amorphous silica present in the specimens. This results in increased ingesting of the C–H phase to produce more C–S–H phases in the matrix. The VA sample shows a more significant decrease in the portlandite (C–H) phase due to the presence of amorphous silica in the sample. This is due to the reactive components such as amorphous silica. When incorporated into concrete, these reactive components can participate in pozzolanic reactions with calcium hydroxide formed during cement hydration. This can lead to the formation of additional cementitious compounds, which may reduce the mass loss during TGA by contributing to the densification of the concrete matrix. Furthermore, at lower temperatures, the presence of reactive components in the VA may contribute to a reduction in mass loss due to pozzolanic reactions. However, at higher temperatures, the decomposition of VA components or interactions with other constituents in the concrete mix may lead to increased mass loss, as shown in Figure 10.

While TGA effectively quantifies $Ca(OH)_2$ and offers insights into pozzolanic reactions, it may not fully detect other phases in VA, such as unreactive silica or crystalline quartz, which can affect concrete properties. Additionally, minerals like feldspar and zeolites may not show clear

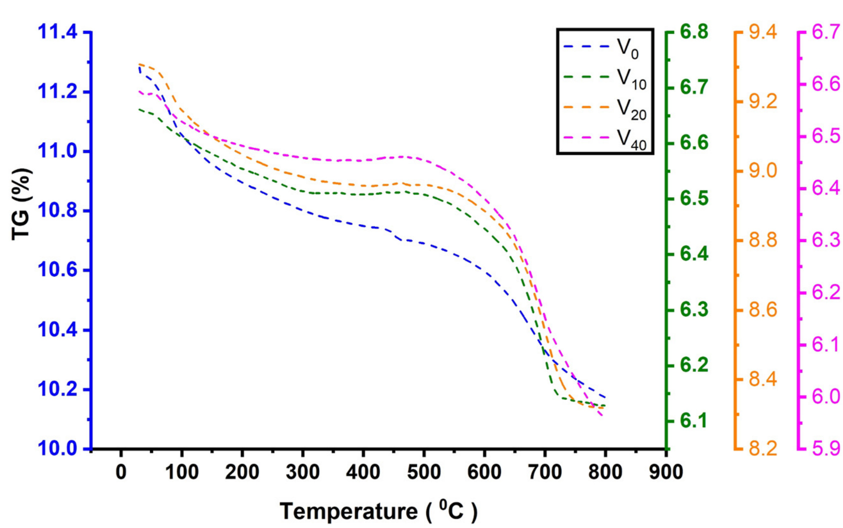

Figure 10: TGA of VA specimens in concrete.

thermal transitions in the TGA range, potentially underestimating their impact on the concrete matrix [82].

XRD complements TGA by detailing the crystalline phases in VA concrete, including portlandite, quartz, and C–S–H. However, it may not quantify amorphous phases, which are common in VA. Thus, using both techniques together is essential for a comprehensive assessment of pozzolanic activity.

From the above discussion, it can be deduced that VA concrete exhibits enhanced thermal stability compared to conventional concrete due to its lower porosity and denser microstructure, resulting from pozzolanic reactions between reactive silica in VA and calcium hydroxide during cement hydration. These reactions create additional C–S–H phases, improving the concrete's structural integrity and thermal performance.

In contrast, conventional concrete has higher porosity, making it more susceptible to thermal degradation and cracking under high temperatures. TGA indicates that VA concrete experiences less mass loss at elevated temperatures, highlighting its improved resistance to heat. Thus, VA concrete is a more reliable choice for applications exposed to high temperatures.

4 Conclusion

The current study aimed to assess the consequence of using ordinary VA as an additional for cement in producing environmentally friendly concrete. The impact of VA on the mechanical characteristics was investigated. XRD and TGA investigations were performed to study how VA impacts the microstructure of the specimens. Below is the conclusion reached from the experimental findings.

- The slump of the VAC decreases with increased concentration ranging from 0 to 40%. This is due to the particle size and shape, water demand, and pozzolanic activity. As the concentration of VA increases, the amount of pozzolanic reaction taking place within the concrete mix also increases. Pozzolanic reactions consume calcium hydroxide and water, forming additional cementitious compounds. This can result in a reduction in the amount of free water available for lubricating the concrete mix, leading to a reduction in slump.
- Concrete density significantly increased by substituting cement with VA, thanks to its pozzolanic activity and micro fillers. The combined impact of the pozzolanic reaction and micro filling of VA enhanced the density characteristics of concrete. A higher dose of VA negatively impacts density because of the lack of flowability. Various researches suggest different optimal dosage adjustments based on the source of vitamin A. The normal optimal dose of VA varies from 10 to 20%.
- The use of VA as a partial cement increases the compressive strengths of the composite. This increase can be attributed to the high pozzolanic reactions in the VA with matrix. The addition of VA up to a concentration of 10% results in an improvement in compressive strength compared to the control specimen. This improvement could be attributed to factors such as pozzolanic activity, particle packing, and enhanced densification of the concrete matrix due to the presence of VA. In addition, a decrease in the matrix is observed after optimal dosage due to unreactive silica, and excessive water demand.
- XRD examination indicated that the presence of 10% VA led to a notable decrease in the concentration of calcium hydroxide, attributed to its superior pozzolanic properties associated with the other mixtures.
- Microstructure SEM analysis reveals that VA particles react with the CH to form a densified C–S–H gel. In addition, deviation of cracks is observed, which is a good sign for strength and durability.
- TGA indicates that specimens with 10% VA exhibit a notable decrease in the portlandite phase due to the high responsiveness of the very tiny formless silica present in the specimens. This leads to increased ingesting of the C–H phase to produce more C–S–H stages in the matrix.

5 Limitations, recommendations, and applications

This study offers significant insights into the potential of VA as an SCM, though it has several limitations. First, while the reduced portlandite phase improves durability by lowering permeability, further research is needed to understand its impact on long-term concrete performance, especially under real-world environmental conditions. Additionally, the experimental setup primarily focused on short-term performance, which may not fully reflect VA concrete's behavior over extended periods. Modifying experimental procedures to incorporate accelerated aging and environmental exposure could provide a more comprehensive view of VA's durability. A key limitation relates to the VA's mineral composition, which may vary by region and influence performance outcomes; future studies should consider this variability for broader applicability. The potential environmental implications of sourcing and processing VA should also be assessed to align with sustainability goals.

Practical applications of VA concrete are promising, particularly in sustainable construction. VA's pozzolanic activity contributes to reducing cement content, lowering CO_2 emissions, and enhancing material durability. This aligns with the industry's broader goals to develop low-carbon, durable building materials. Expanding this research to evaluate VA in other CCs could further contribute to sustainable construction practices. Future work could explore the environmental life-cycle impact of VA-based concrete, especially for infrastructure exposed to harsh conditions.

Acknowledgments: The authors extend their appreciation to the Deanship of Scientific Research at King Khalid University for funding this work through a large group Research Project under grant number RGP2/72/44.

Funding information: The authors extend their appreciation to the Deanship of Scientific Research at King Khalid University for funding this work through a large group Research Project under grant number RGP2/72/44.

Author contributions: All authors have accepted responsibility for the entire content of this manuscript and approved its submission.

Conflict of interest: The authors state no conflict of interest.

Data availability statement: The datasets generated and/or analyzed during the current study are available from the corresponding author on reasonable request.

References

[1] Griffiths, S., B. K. Sovacool, D. D. Del Rio, A. M. Foley, M. D. Bazilian, J. Kim, et al. Decarbonizing the cement and concrete industry: A systematic review of socio-technical systems, technological innovations, and policy options. *Renewable and Sustainable Energy Reviews*, Vol. 1980, 2023, id. 113291.

[2] Vázquez-Calle, K., V. Guillén-Mena, and F. Quesada-Molina. Analysis of the embodied energy and CO2 emissions of ready-mixed concrete: a case study in Cuenca, Ecuador. *Materials*, Vol. 15, 2022, id. 4896.

[3] Dong, J. F., Y. Xu, Z. W. Guan, and Q. Y. Wang. Freeze-thaw behaviour of basalt fibre reinforced recycled aggregate concrete filled CFRP tube specimens. *Engineering Structures*, Vol. 273, 2022, id. 115088.

[4] Kang, F., Y. Wu, J. Ma, and J. Li. Structural identification of super high arch dams using Gaussian process regression with improved salp swarm algorithm. *Engineering Structures*, Vol. 286, 2023, id. 116150.

[5] Marsh, A. T. M., A. P. M. Velenturf, and S. A. Bernal. Circular Economy strategies for concrete: implementation and integration. *Journal of Cleaner Production*, Vol. 362, 2022, id. 132486.

[6] Hottle, T., T. R. Hawkins, C. Chiquelin, B. Lange, B. Young, P. Sun, et al. Environmental life-cycle assessment of concrete produced in the United States. *Journal of Cleaner Production*, Vol. 363, 2022, id. 131834.

[7] Ntuli, M. N., M. O. Dioha, D. R. E. Ewim, and A. C. Eloka-Eboka. Review of energy modelling, energy efficiency models improvement and carbon dioxide emissions mitigation options for the cement industry in South Africa. *Mater Today Proceedings*, Vol. 65, 2022, pp. 2260–2268.

[8] Chaudhury, R., U. Sharma, P. C. Thapliyal, and L. P. Singh. Low-CO_2 emission strategies to achieve net zero target in cement sector. *Journal of Cleaner Production*, Vol. 417, 2023, id. 137466.

[9] Turner, L. K. and F. G. Collins. Carbon dioxide equivalent (CO_2-e) emissions: A comparison between geopolymer and OPC cement concrete. *Construction and Building Materials*, Vol. 43, 2013, pp. 125–130.

[10] Chen, D., F. Kang, J. Chen, S. Zhu, and H. Li. Effect of light source wavelength on surface defect imaging in deep-water concrete dams. *NDT and E International*, Vol. 147, 2024, id. 103198.

[11] Liu, Y., B. Wang, Y. Fan, J. Yu, T. Shi, Y. Zhou, et al. Effects of reactive MgO on durability and microstructure of cement-based materials: Considering carbonation and pH value. *Construction and Building Materials*, Vol. 426, 2024, id. 136216.

[12] Samimi, K., S. Kamali-Bernard, A. Akbar Maghsoudi, M. Maghsoudi, and H. Siad. Influence of pumice and zeolite on compressive strength, transport properties and resistance to chloride penetration of high strength self-compacting concretes. *Construction and Building Materials*, Vol. 151, 2017, pp. 292–311.

[13] Ashish, D. K. Concrete made with waste marble powder and supplementary cementitious material for sustainable development. *Journal of Cleaner Production*, Vol. 211, 2019, pp. 716–729.

[14] Thomas, B. S., J. Yang, K. H. Mo, J. A. Abdalla, R. A. Hawileh, and E. Ariyachandra. Biomass ashes from agricultural wastes as supplementary cementitious materials or aggregate replacement in cement/geopolymer concrete: A comprehensive review. *Journal of Building Engineering*, Vol. 40, 2021, id. 102332.

[15] Liu, Y., J. Dong, S. Yuan, K. Li, X. Hu, and Q. Wang. Variable fatigue loading effects on corrugated steel box girders with recycled concrete. *J Constr Steel Res*, Vol. 215, 2024, id. 108526.

[16] Fang, B., Z. Qian, Y. Song, X. Diao, T. Shi, X. Cai, et al. Evaluation of early crack resistance performance of concrete mixed with ternary minerals using temperature stress testing machine (TSTM). *Journal of Cleaner Production*, Vol. 465, 2024, id. 142780.

[17] He, L., B. Chen, Q. Liu, H. Chen, H. Li, W. T. Chow, et al. A quasi-exponential distribution of interfacial voids and its effect on the interlayer strength of 3D printed concrete. *Additive Manufacturing*, Vol. 89, 2024, id. 104296.

[18] Sun, L., C. Wang, C. Zhang, Z. Yang, C. Li, and P. Qiao. Experimental investigation on the bond performance of sea sand coral concrete with FRP bar reinforcement for marine environments. *Advances in Structural Engineering*, Vol. 26, No. 3, 2023, pp. 533–546.

[19] Huang, H., Y. Yuan, W. Zhang, and M. Li. Seismic behavior of a replaceable artificial controllable plastic hinge for precast concrete beam-column joint. *Engineering Structures*, Vol. 245, 2021, id. 112848.

[20] Arif, M., F. Jan, A. Rezzoug, M. A. Afridi, M. Luqman, W. A. Khan, et al. Data-driven models for predicting compressive strength of 3D-printed fiber-reinforced concrete using interpretable machine learning algorithms. *Case Studies in Construction Materials*, Vol. 21, 2024, id. e03935.

[21] Asif, U., M. F. Javed, D. M. Alsekait, D. S. AbdElminaam, and H. Alabduljabbar. Toward sustainability: Integrating experimental study and data-driven modeling for eco-friendly paver blocks containing plastic waste. *Reviews on Advanced Materials Science*, Vol. 63, No. 1, 2024, id. 20240051.

[22] Huang, H., M. Li, W. Zhang, and Y. Yuan. Seismic behavior of a friction-type artificial plastic hinge for the precast beam–column connection. *Archives of Civil and Mechanical Engineering*, Vol. 22, No. 4, 2022, id. 201.

[23] Shilar, F. A., S. V. Ganachari, and V. B. Patil. Investigation of the effect of granite waste powder as a binder for different molarity of geopolymer concrete on fresh and mechanical properties. *Materials Letters*, Vol. 309, 2022, id. 131302.

[24] Shilar, F. A., S. V. Ganachari, and V. B. Patil. Advancement of nano-based construction materials-A review. *Construction and Building Materials*, Vol. 359, 2022, id. 129535.

[25] Shilar, F. A., S. V. Ganachari, V. B. Patil, I. Neelakanta Reddy, and J. Shim. Preparation and validation of sustainable metakaolin based geopolymer concrete for structural application. *Construction and Building Materials*, Vol. 371, 2023, id. 130688.

[26] Yang, M., S. R. Paudel, and E. Asa. Comparison of pore structure in alkali activated fly ash geopolymer and ordinary concrete due to alkali-silica reaction using micro-computed tomography. *Construction and Building Materials*, Vol. 236, 2020, id. 117524.

[27] Ishak, S., H. S. Lee, J. K. Singh, M. A. Ariffin, N. H. Lim, and H. M. Yang. Performance of fly ash geopolymer concrete incorporating bamboo ash at elevated temperature. *Materials*, Vol. 12, 2019, id. 3404.

[28] Zhao, R., Y. Yuan, Z. Cheng, T. Wen, J. Li, F. Li, et al. Freeze-thaw resistance of Class F fly ash-based geopolymer concrete. *Construction and Building Materials*, Vol. 222, 2019, pp. 474–483.

[29] Ahmad, S., O. S. Baghabra Al-Amoudi, S. M. S. Khan, and M. Maslehuddin. Effect of silica fume inclusion on the strength, shrinkage and durability characteristics of natural pozzolan-based cement concrete. *Case Studies in Construction Materials*, Vol. 17, 2022, id. e01255.

[30] Okoye, F. N., S. Prakash, and N. B. Singh. Durability of fly ash based geopolymer concrete in the presence of silica fume, *Journal of cleaner Production*, Vol. 149, 2017, pp. 1062–1067.

[31] Fahmy, M., M. Abu El-Hassan, G. Kamh, and A. Bashandy. Investigation of using nano-silica, silica fume and fly ash in high strength concrete. *ERJ. Engineering Research Journal*, Vol. 43, 2020, pp. 211–221.

[32] Sosa, I., C. Thomas, J. A. Polanco, J. Setién, J. A. Sainz-Aja, and P. Tamayo. Durability of high-performance self-compacted concrete using electric arc furnace slag aggregate and cupola slag powder. *Cement and Concrete Composites*, Vol. 127, 2022, id. 104399.

[33] Su, Y., P. Jin, and Q. Zhan. Improvement in mechanical properties and microstructure of electric arc furnace slag bricks by microbial accelerated carbonation. *Journal of Sustainable Cement-Based Materials*, Vol. 12, No. 8, 2023, pp. 1033–1047.

[34] Chen, D., F. Kang, J. Li, S. Zhu, and X. Liang. Enhancement of underwater dam crack images using multi-feature fusion. *Automation in Construction*, Vol. 167, 2024, id. 105727.

[35] Iftikhar, B., S. C. Alih, M. Vafaei, M. A. Elkotb, M. Shutaywi, M. F. Javed, et al. Predictive modeling of compressive strength of sustainable rice husk ash concrete: Ensemble learner optimization and comparison. *Journal of Cleaner Production*, Vol. 348, 2022, id. 131285.

[36] Yao, W., M. Bai, J. Pang, and T. Liu. Performance degradation and damage model of rice husk ash concrete under dry–wet cycles of sulfate environment. *Environmental Science and Pollution Research*, Vol. 29, 2022, pp. 59173–59189.

[37] Li, Q. and Z. Song. Prediction of compressive strength of rice husk ash concrete based on stacking ensemble learning model. *Journal of Cleaner Production*, Vol. 382, 2023, id. 135279.

[38] Althoey, F., O. Zaid, R. Martínez-García, J. de Prado-Gil, M. Ahmed, and A. M. Yosri. Ultra-high-performance fiber-reinforced sustainable concrete modified with silica fume and wheat straw ash. *Journal of Materials Research and Technology*, Vol. 24, 2023, pp. 6118–6139.

[39] Shar, I. A., F. A. Memon, N. Bheel, O. Benjeddou, and M. Alwetaishi. Effect of used engine oil on the mechanical properties and embodied carbon of concrete blended with wheat straw ash as cementitious material. *Environmental Science and Pollution Research*, Vol. 30, 2023, pp. 75879–75893.

[40] Zaid, O., R. Martínez-García, and F. Aslam. Influence of wheat straw ash as partial substitute of cement on properties of high-strength concrete incorporating graphene oxide. *Journal of Materials in Civil Engineering*, Vol. 34, No. 11, 2022, id. 04022295.

[41] Rizwan Hussain, R., A. M. Alhozaimy, and A. Al-Negheimish. Role of scoria natural pozzolan in the passive film development for steel rebars in chloride-contaminated concrete environment. *Construction and Building Materials*, Vol. 357, 2022, id. 129335.

[42] Shilar, F. A., S. V. Ganachari, V. B. Patil, N. Almakayeel, and T. M. Y. Khan. Development and optimization of an eco-friendly geopolymer brick production process for sustainable masonry construction. *Case Studies in Construction Materials*, Vol. 18, 2023, id. e02133.

[43] Shilar, F. A., S. V. Ganachari, V. B. Patil, T. M. Y. Khan, S. Javed, and R. U. Baig. Optimization of alkaline activator on the strength properties of geopolymer concrete. *Polymers*, Vol. 14, 2022, id. 2434.

[44] Shilar, F. A., S. V. Ganachari, V. B. Patil, K. S. Nisar, A. H. Abdel-Aty, and I. S. Yahia. Evaluation of the effect of granite waste powder by varying the molarity of activator on the mechanical properties of ground granulated blast-furnace slag-based geopolymer concrete. *Polymers*, Vol. 14, 2022, id. 306.

[45] Shilar, F. A., S. V. Ganachari, V. B. Patil, S. Javed, T. M. Y. Khan, and R. U. Baig. Assessment of destructive and nondestructive analysis for GGBS based geopolymer concrete and its statistical analysis. *Polymers*, Vol. 14, 2022, id. 3132.

[46] Dong, J. F., Q. Y. Wang, Z. W. Guan, and H. K. Chai. High-temperature behaviour of basalt fibre reinforced concrete made with recycled aggregates from earthquake waste. *Journal of Building Engineering*, Vol. 48, 2022, id. 103895.

[47] Chakkamalayath, J., M. Abdulsalam, and S. Al-Bahar. Compatibility of superplasticizers with cement paste and concrete mixes containing Type I and Type V cement, and volcanic ash. *Innovative Infrastructure Solutions*, Vol. 7, 2022, pp. 1–13.

[48] Alqarni, A. S. A comprehensive review on properties of sustainable concrete using volcanic pumice powder ash as a supplementary cementitious material. *Construction and Building Materials*, Vol. 323, 2022, id. 126533.

[49] Siddique, R. Properties of concrete made with volcanic ash. *Resources, Conservation and Recycling*, Vol. 66, 2012, pp. 40–44.

[50] Zeyad, A. M., B. A. Tayeh, and M. O. Yusuf. Strength and transport characteristics of volcanic pumice powder based high strength concrete. *Construction and Building Materials*, Vol. 216, 2019, pp. 314–324.

[51] Cimesa, M. and M. A. Moustafa. Experimental characterization and analytical assessment of compressive behavior of carbon nanofibers enhanced UHPC. *Case Studies in Construction Materials*, Vol. 17, 2022, id. e01487.

[52] Afridi, H. F., D. Khan, W. A. Khan, H. Jamal, A. A. Durrani, M. A. Afridi, et al. Utilizing waste engine oil and Sasobit to improve the rheological and physiochemical properties of RAP. *Discover Civil Engineering*, Vol. 1, No. 1, 2024, id. 131.
[53] Wang, X. Y. Evaluation compressive strength of cement-limestone-slag ternary blended concrete using artificial neural networks (ANN) and gene expression programming (GEP). *Key Engineering Materials KEM*, Vol. 837, 2020, pp. 119–124.
[54] Singh, N. B. and B. Middendorf. Geopolymers as an alternative to Portland cement: An overview. *Construction and Building Materials*, Vol. 237, 2020, id. 117455.
[55] Afridi, M. A., Y. Wu, M. J. Khattak, and F. Karbalaeisaleh. Development of a highly conductive nano-engineered geopolymer for geothermal applications. *ASME Open Journal of Engineering*, Vol. 1, 2024.
[56] Keshta, M. M., M. M. Y. Elshikh, M. Abd Elrahman, and O. Youssf. Utilizing of magnetized water in enhancing of volcanic concrete characteristics. *Journal of Composites Science*, Vol. 6, No. 10, 2022, id. 320.
[57] Szabó, R., F. Kristály, S. Nagy, R. Singla, G. Mucsi, and S. Kumar. Reaction, structure and properties of eco-friendly geopolymer cement derived from mechanically activated pumice. *Ceramics International*, Vol. 49, 2023, pp. 6756–6763.
[58] Waqar, A., N. Bheel, N. Shafiq, I. Othman, M. B. Khan, M. S. Mansoor, et al. Effect of volcanic pumice powder ash on the properties of cement concrete using response surface methodology. *Journal of Building Pathology and Rehabilitation*, Vol. 8, No. 1, 2023, id. 17.
[59] Sebayang, M. D. Analyze the proportion of volcanic ash of Sinabung volcano at the most optimum to get the compressive strength and tensile strength of concrete. *In IOP Conference Series: Materials Science and Engineering*, Institute of Physics Publishing, 2020.
[60] Karolina, R. and M. P. Simanjuntak. The influence of using volcanic ash and lime ash as filler on compressive strength in self compacting concrete. *In IOP Conference Series: Earth and Environmental Science*, Institute of Physics Publishing, 2018, p. 12038.
[61] Hossain, K. M. A. and M. Lachemi. Strength, durability and microstructural aspects of high performance volcanic ash concrete. *Cement and Concrete Research*, Vol. 37, 2007, pp. 759–766.
[62] Khan, K., M. N. Amin, M. Usman, M. Imran, M. A. Al-Faiad, and F. I. Shalabi. Effect of fineness and heat treatment on the pozzolanic activity of natural volcanic ash for its utilization as supplementary cementitious materials. *Crystals (Basel)*, Vol. 12, 2022, id. 302.
[63] Abdullah, G. M. S., I. M. H. Alshaikh, A. M. Zeyad, H. M. Magbool, and B. H. A. Bakar. The effect of openings on the performance of self-compacting concrete with volcanic pumice powder and different steel fibers. *Case Studies in Construction Materials*, Vol. 17, 2022, id. e01148.
[64] Al-Fadala, S., J. Chakkamalayath, S. Al-Bahar, A. Al-Aibani, and S. Ahmed. Significance of performance based specifications in the qualification and characterization of blended cement using volcanic ash. *Construction and Building Materials*, Vol. 144, 2017, pp. 532–540.
[65] Kabay, N., M. M. Tufekci, A. B. Kizilkanat, and D. Oktay. Properties of concrete with pumice powder and fly ash as cement replacement materials. *Construction and Building Materials*, Vol. 85, 2015, pp. 1–8.
[66] Celik, K., M. D. Jackson, M. Mancio, C. Meral, A. H. Emwas, P. K. Mehta, et al. High-volume natural volcanic pozzolan and limestone powder as partial replacements for portland cement in self-compacting and sustainable concrete. *Cement and Concrete Composites*, Vol. 45, 2014, pp. 136–147.
[67] Al-Bahar, S., J. Chakkamalayath, A. Joseph, M. Abdulsalam, S. Al-Otaibi, and A. Al-Aibani. Effect of volcanic ash incorporation on the mechanical properties and surface morphology of hydrated cement paste. *Journal of Materials in Civil Engineering*, Vol. 29, No. 8, 2017, id. 04017052.
[68] Hossain, K. M. A. and M. Lachemi. Development of volcanic ash concrete: Strength, durability, and microstructural investigations. *ACI Materials Journal*, Vol. 103, 2006, pp. 11–17.
[69] Hossain, K. M. A. and M. Lachemi. Fresh, mechanical, and durability characteristics of self-consolidating concrete incorporating volcanic ash. *Journal of Materials in Civil Engineering*, Vol. 22, 2010, pp. 651–657.
[70] Liu, X., M. Zhang, L. Shao, and Z. Chen. Effect of volcanic ash filler on thermal viscoelastic property of SBS modified asphalt mastic. *Construction and Building Materials*, Vol. 190, 2018, pp. 495–507.
[71] ASTM C150/C150M, Standard Specification for Portland Cement C150/C150M, 2019.
[72] ASTM, ASTM C128. Standard Test Method for Relative Density (Specific Gravity) and Absorption of Fine Aggregate. *Annual Book of ASTM Standards*, 2022, pp. 1–6.
[73] ASTM C143/C143M. *Standard Test Method for Slump of Hydraulic-Cement Concrete, Astm C143*, 2015, pp. 1–4.
[74] ASTM International. *ASTM Standard C39/C39M-16, Standard Test Method for Compressive Strength of Cylindrical Concrete Specimens*, ASTM International, 2016.
[75] ASTM C642. *Standard Test Method for Density, Absorption, and Voids in Hardened Concrete*, ASTM, ASTM International, 2013, pp. 1–3.
[76] ASTM C618-17a. Standard specification for coal fly ash and raw or calcined natural pozzolan for use in concrete. *Annual Book of ASTM Standards*, 2017, pp. 1–5.
[77] Khan, K., M. A. M. Johari, M. N. Amin, and M. Nasir. Development and evaluation of basaltic volcanic ash based high performance concrete incorporating metakaolin, micro and nano-silica. *Developments in the Built Environment*, Vol. 17, 2024, id. 100330.
[78] Kabay, N. and F. Aköz. Effect of prewetting methods on some fresh and hardened properties of concrete with pumice aggregate. *Cement and Concrete Composites*, Vol. 34, 2012, pp. 503–507.
[79] Silva, Y. F., D. A. Lange, and S. Delvasto. Effect of incorporation of masonry residue on the properties of self-compacting concretes. *Construction and Building Materials*, Vol. 196, 2019, pp. 277–283.
[80] Petrounias, P., P. P. Giannakopoulou, A. Rogkala, A. Papalla, V. Giamas, P. Lampropoulou, et al. The effect of the microstructure of diabases from greece and cyprus on their engineering characteristics and the mechanical behaviour of concrete. *Buildings*, Vol. 13, 2023, id. 396.
[81] Hamada, H. M., F. Abed, S. Beddu, A. M. Humada, and A. Majdi. Effect of Volcanic Ash and Natural Pozzolana on mechanical properties of sustainable cement concrete: A comprehensive review. *Case Studies in Construction Materials*, Vol. 19, 2023, id. e02425.
[82] Ali, A., Y. W. Chiang, and R. M. Santos. X-ray diffraction techniques for mineral characterization: a review for engineers of the fundamentals, applications, and research directions. *Minerals*, Vol. 12, 2022, id. 205.